NO oxidation on Fe- and Cu-zeolites mixed with BaO/Al$_2$O$_3$: Free oxidation regime and relevance for the NH$_3$-SCR chemistry at low temperature

Tommaso Selleri, Federica Gramigni, Isabella Nova, Enrico Tronconi*

Dipartimento di Energia, Laboratorio di Catalisi e Processi Catalitici, Politecnico di Milano, Via La Masa 34, I-20156, Milano, Italy
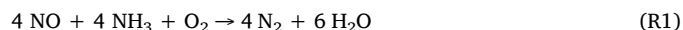
ABSTRACT

Oxidative activation of NO is commonly regarded as a key step in the low-temperature mechanism of Standard SCR on metal-promoted zeolite catalysts for NH$_3$-SCR of NOx. In the present work, we systematically investigate the dynamics of NO oxidation as well as the reactivity of NO + NO$_2$ with adsorbed and gas-phase NH$_3$ on Fe-ZSM-5 and Cu-CHA catalysts, using chemical trapping techniques. The approach is based on physically mixing the metal promoted zeolite catalyst with a NOx trap material, i.e. BaO/Al$_2$O$_3$. We show that in these combined systems, as long as NOx storage sites are available, the initial rate of NO oxidative activation is substantially higher than over the metal promoted zeolite alone, as measured in conventional steady-state activity tests for NO oxidation to NO$_2$. Similar dynamics with enhanced initial NO conversions are observed also in the case of metal promoted zeolite catalysts with preadsorbed NH$_3$, suggesting a close analogy between the role of BaO in the chemical trapping runs and the role of adsorbed NH$_3$ in Standard SCR conditions, both species removing effectively the NO oxidation products from the gas phase and therefore preventing their inhibitory action. These novel findings are relevant to estimate correctly the intrinsic kinetics of the NO oxidative activation over metal-promoted zeolite SCR catalysts, and may help to explain the so far unresolved divergence between the rate of NO oxidation to NO$_2$ and the rate of the Standard SCR reaction. We show, in fact, that the rate of uninhibited NO oxidation is able to sustain the Standard SCR activity over both Fe- and Cu-zeolite catalysts.

1. Introduction

The oxidative activation of NO on metal (Cu, Fe) promoted zeolite catalysts is widely believed [1–8] to be a fundamental step in the Standard Selective Catalytic Reduction (SCR) of NO with NH$_3$,

$$4\,NO + 4\,NH_3 + O_2 \rightarrow 4\,N_2 + 6\,H_2O \qquad (R1)$$

i.e. the main reaction involved in the Urea-SCR technology for the abatement of NOx from Diesel exhausts. Despite such a general agreement, however, a comprehensive and satisfactory account for the Standard SCR reaction mechanism is still lacking: the recent literature shows a continuous evolution of the proposals for the related catalytic cycle [9–15], all of them still involving different intermediates and diverging pseudo-elementary steps.

Historically, some of the early mechanistic models proposed the NO to NO$_2$ oxidation to be rate determining (RDS) for Standard SCR [1,3,4,16]. In this two-step sequence, gaseous NO$_2$ acts as a highly reactive intermediate, subsequently reacting rapidly with additional NO and NH$_3$ via the Fast SCR mechanism. However, several groups, including ours, have highlighted that, in many situations, the rates of NO

oxidation to NO$_2$ and of Standard SCR over metal promoted zeolite catalysts do not correlate. In particular, on Cu-promoted zeolite catalysts the NO oxidation to NO$_2$ is significantly slower than the NO conversion via Standard SCR, an observation apparently in strong contrast with the above proposed mechanism [8,17]. On the opposite, on Fe-promoted zeolites the NO oxidation rate can even overcome the Standard SCR rate [8], again challenging the hypothesis of a sequential scheme unless invoking an additional inhibition effect (e.g. due to NH$_3$).

In a recent chemical trapping study [18], aimed at the identification of the NOx intermediates in the Standard SCR mechanism, we have shown that a crucial redox step in the NO oxidative activation involves the oxidation of the N atom of NO to a state of $+3$. We have also shown that this may be in line with the formation of NO$_2$ which, in excess NO, behaves essentially as a nitrite precursor [19], possibly in the form of N$_2$O$_3$. Nevertheless, it is still not clear how to reconcile the fact that the Standard SCR reaction might involve the oxidative activation of NO to NO$_2$, with the aforementioned kinetic argument [8].

In the present work we use chemical trapping techniques [20–22] to investigate the dynamics and the transient kinetics of the oxidative

activation of NO at low temperature on Fe- and Cu-promoted zeolites + BaO/Al$_2$O$_3$ combined systems, tested in spatial arrangements with different degrees of separation, i.e. either as individual phases, or in segregated (sequential) beds, or as a physical mixture. In an effort to relate our results to the Standard SCR mechanism, we also run comparative NO oxidation experiments over the Fe- and Cu-zeolite catalysts with preadsorbed ammonia.

The results reveal for the first time important differences between the steady-state NO oxidation rates and the initial rates of the NO oxidative activation, in the case of both metal-promoted zeolites mixed with BaO/Al$_2$O$_3$ and of the individual catalysts preloaded with ammonia, which may pave the way to new insights in the Standard SCR catalytic chemistry.

2. Experimental

Different systems comprising a Fe-ZSM-5 zeolite (22 mg), a Cu-CHA zeolite (16 mg) and in-house prepared BaO/Al$_2$O$_3$ (44 mg), all in the form of powders, were tested in different spatial arrangements. The Fe-ZSM-5 was a commercial catalyst manufactured by Zeolyst (CP 7117), with a SiO$_2$/Al$_2$O$_3$ ratio of 24, surface area of 300 m^2/g and 1% w/w Fe content (estimated Fe/Al = 0.136). The Cu-CHA sample was a commercial material, with a SiO$_2$/Al$_2$O$_3$ ratio of 25 and 2% w/w Cu content (estimated Cu/Al = 0.253). The two selected SCR catalysts show the typical performances of these classes of materials with NO conversions in Standard SCR (Q = 120 Ncc/min, H$_2$O = 0%, O$_2$ = 2%, T = 200 °C, NH$_3$ = NO = 500 ppm) and NO oxidation (Q = 120 Ncc/min, H$_2$O = 0%, O$_2$ = 2%, T = 200 °C. NO = 500 ppm) at 200 °C of 0.21/ 0.1 and 0.33/0.008 (Fe-ZSM-5 and Cu-CHA, respectively). Both zeolite powders were dried at 120 °C for 1 h and sieved to 120–140 mesh (average particle size = 115 μm). The BaO/Al$_2$O$_3$ component (Ba content = 16% w/w) was prepared in-house by incipient wetness impregnation, using aqueous solutions of Ba(CH$_3$COO)$_2$ (Sigma Aldrich, 99% pure) to impregnate the γ-alumina support (Versal 250 from Eurosupport: surface area = 200 m^2/g and pore volume = 1.2 cm^3/g) calcined at 800 °C. After impregnation, the powder was dried at 80 °C overnight, calcined at 500 °C for 5 h, and sieved to 140–200 mesh (average particle size = 90 μm). Cordierite with 120–140 mesh size was added for dilution. In all runs, the powders were loaded in a quartz microflow reactor (ID = 7 mm). The following configurations have been tested: i) a physical mixture of Fe-ZSM-5 or Cu-CHA and BaO/Al$_2$O$_3$ powders (identified in the following as Fe-Ba-MM and Cu-Ba-MM, respectively) with the two phases in loose contact and a total dilution with cordierite up to 120 mg; ii) a double-bed configuration with Fe-ZSM-5 upstream, followed by a BaO/Al$_2$O$_3$ layer (identified in the following as Fe-Ba-DB); iii) the single catalysts (Fe-ZSM-5 or Cu-CHA) tested individually after dilution up to a total bed load of 120 mg.

Before running every test, each new sample was conditioned once for 5 h at 600 °C in a continuous flow of 10% v/v H$_2$O and 10% v/v O$_2$ in He. Moreover, prior to every experiment, a reductive pretreatment was performed feeding 500 ppm of NO and NH$_3$ at 550 °C continuously for 1 h, followed by a cool-down transient to the test temperature in inert He. The feed mixture to the reactor was composed from calibrated NO + He, NO$_2$ + He, NH$_3$ + He, O$_2$ + He mixtures in gas bottles using several mass flow controllers (Brooks Instruments). NO and O$_2$ were fed to the reactor via independent lines and mixed just before the reactor inlet to prevent formation of NO$_2$ upstream of the catalyst bed. The purity of the mixtures was checked by a UV analyzer during preliminary calibrations. The gas species concentrations at the reactor outlet were analyzed by a quadrupole mass spectrometer (Balzers QMS 200) and a UV analyzer (ABB LIMAS 11 HW) arranged in a parallel configuration.

The experimental protocol herein adopted is in line with the one described and validated in our previous works [20–22]. In general, two different types of transient experiments were performed at different temperatures: i) stepwise addition of 2% O$_2$ in a continuous flow of 500 ppm of NO in He on prereduced samples; ii) stepwise addition of

2% O$_2$ in a continuous flow of 500 ppm of NO on prereduced samples previously saturated with NH$_3$. In addition, Standard SCR experiments varying the NH$_3$ feed concentration were performed on both Fe-ZSM-5 and Cu-CHA samples: in a continuous flow of 500 ppm NO and 2% O$_2$, the NH$_3$ feed concentration was stepwise changed from 500 ppm down to 100 or 125 ppm, waiting for the corresponding steady states. All the tests were run with an overall volumetric flow rate of 120 cm^3/min (STP) at a constant adsorption temperature under dry conditions. Our previous work, in fact, pointed out a strong negative impact of H$_2$O on the amount of NOx trapped on BaO, due to its inhibitory action both on the NO oxidation activity of metal promoted zeolites [23], as also well known in the literature, and on the nitrites storage on BaO, documented e.g. by a dedicated experiment in [21]. The overall amount of stored species was calculated from the integral of the NOx concentration profile until the NO$_2$ concentration reached steady state. In this way we also try to avoid possibility of nitrites conversion to nitrates by NO$_2$, as reported in literature [18].

Additional details regarding the experimental set-up and procedures, as well as the preparation and the characterization of the tested samples, can be found in [20–22].

3. Results and discussion

3.1. Uninhibited NO oxidation regime in the presence of BaO/Al$_2$O$_3$

Fig. 1 shows the stepwise feed of 2% O$_2$ while continuously feeding 500 ppm of NO at constant temperature (200 °C) on the Fe-ZSM–5 + BaO/Al$_2$O$_3$ system in different configurations. This is an extension of a similar experiment reported in another recent work from our group [18]. Notice that, for all the three cases, as soon as O$_2$ is fed to the reactor there is a small and fast perturbation in the NO signal, possibly due to a non-instantaneous valve switching. No adsorption – reactivity of NO alone is detected at these conditions for all the three considered systems. In the case of Fe-ZSM-5 alone (dotted lines), as soon as O$_2$ is introduced NO is converted to NO$_2$, in agreement with the well-known NO oxidation reaction (R2),

$$NO + \tfrac{1}{2}\,O_2 \leftrightarrow NO_2 \tag{R2}$$

The system rapidly reaches a steady state in which about 50 ppm of NO$_2$ are formed, in line with previous results [8]. However, if a layer of BaO/Al$_2$O$_3$ is added after the Fe-zeolite bed (dashed lines), a different behavior is noticed. In the double-bed segregated configuration NO reaches a first pseudo-steady state concentration level (about 400 ppm), which corresponds exactly to twice the NO consumption approached in the following steady state, i.e. the same of the Fe-zeolite only case, as also confirmed by integral calculations of the overall NO conversion until steady state is reached: 8.4 μmol (NOx stored on Fe-Ba-DB) vs
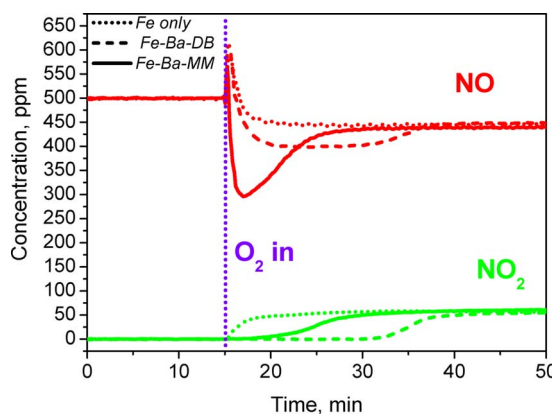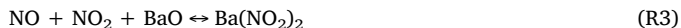

Fig. 1. O$_2$ step feed during NO isothermal adsorption (T = 200 °C; NO = 500 ppm; O$_2$ = 2%) on Fe-ZSM-5 only (dotted lines), Fe-ZSM–5 + BaO/Al$_2$O$_3$ double bed (dashed lines) [18], Fe-ZSM–5 + BaO/Al$_2$O$_3$ mechanical mixture (solid lines).

4.7 μmol (NO oxidized on Fe only). This is in line with the storage of nitrites on BaO/Al$_2$O$_3$ via reactions (R2) and (R3) below:

NO + ½ O$_2$ → NO$_2$ (R2)

NO + NO$_2$ + BaO ↔ Ba(NO$_2$)$_2$ (R3)

Notice that, as confirmed by previous work, BaO/Al$_2$O$_3$ exhibits essentially no activity in the oxidative activation of NO at this temperature [18,20–22]. Furthermore, in the double bed configuration, due to the phase segregation, the NO oxidation activity of the Fe-ZSM-5 catalyst is not modified by BaO, being the additional NO consumption just related to the storage process (R3), which proceeds in the downstream BaO/Al$_2$O$_3$ bed, while reaction (R2) proceeds in the upstream Fe-zeolite bed at the same rate as in the single catalyst base case.

More interestingly, however, a very peculiar transient is observed when Fe-ZSM-5 is combined with BaO/Al$_2$O$_3$ in a physical mixture (solid lines). In this case, the NO outlet concentration temporal profile in Fig. 1 shows a dip of approximately 200 ppm, i.e. indicating that the initial NO oxidation rate is significantly more pronounced than in the steady state oxidation and double bed cases. Very likely, mixing the two phases enables to trap effectively on BaO gaseous intermediates or products of the NO oxidative activation, such as HONO or NO$_2$, as soon as they are formed, thus promoting a "free oxidation" regime wherein the oxidation activity is not (or less) kinetically hindered by the presence of its products (NO$_2$), as happens instead in the steady-state case, in line with literature reports emphasizing the inhibition effects of the NO oxidation products [2,24]. Notice that the lowest point of the NO dip corresponds to much more than twice the NO consumed at steady state in NO oxidation, so this time it is not possible to explain the additional NO conversion simply as the sum of the steady state NO oxidation plus an additional NO consumption for nitrites adsorption on BaO ((R2) + (R3)). Interestingly, the overall NO dip area, being essentially controlled by the amount of NOx storage material, is very similar to the double bed case (8.1 μmol vs 8.4 μmol). Likewise, the final steady state oxidation activity is not modified by the BaO/Al$_2$O$_3$ addition.

Fig. 2 shows the results of the same experiments in the case of the Cu-CHA + BaO/Al$_2$O$_3$ system in the two most relevant configurations (Cu-CHA only and mechanical mixture). Even if with slightly different and generally faster dynamics, the macroscopic behavior is in line with that observed on the Fe-ZSM-5 based systems, Fig. 1: the initial NO oxidation activity to NO$_2$ (215 ppm) on the MM configuration is remarkably higher than the one measured at steady state (about 5 ppm of NO converted) over both MM and single Cu-CHA systems. Here, the enhancement of the NO oxidation activity over steady-state associated with the physical mixture (about 40 times) is even remarkably greater than on the Fe-zeolite system (about 4 times). In addition, the NO dip
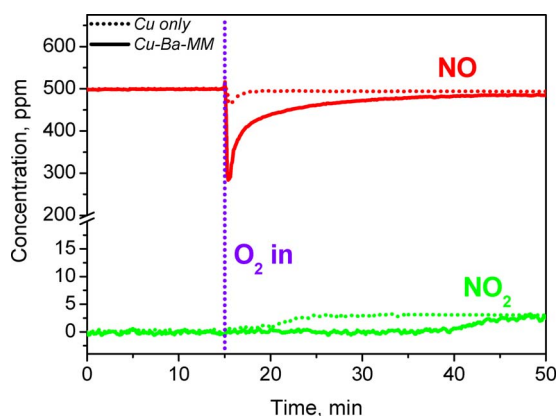
dynamics are significantly sharper and faster than on the Fe-ZSM-5-based system, despite the lower test temperature.

Apparently, this suggests that the oxidative activation of NO on the Cu-zeolite catalyst may be more strongly self-inhibited than on Fe-ZSM-5 and that, under inhibition-free conditions, the NO oxidation rate on Cu-CHA is possibly higher than measured on Fe-ZSM-5, despite the lower NO conversions at steady state, as also discussed in more details later. The overall amount of stored nitrites, calculated according to the standard procedure described in the experimental section, is 6.1 μmol. This is less than the corresponding amount stored on the Fe-ZSM–5 + BaO/Al$_2$O$_3$ system at higher temperature: a possible explanation will be given in the next section.

Summarizing, the present results strongly suggest that, over metal-promoted zeolite SCR catalysts physically mixed with BaO/Al$_2$O$_3$, free NO oxidation proceeds with significantly faster rates than in steady-state NO oxidation runs due to a reduced self-inhibition, as a result of very low NO$_2$ gas-phase concentration (below the detection limit of 5 ppm). Such an enhancement of the NO oxidation rate is found to be especially pronounced on the Cu-CHA catalyst.

3.2. Effect of temperature on the free NO oxidation in the presence of BaO/Al$_2$O$_3$

The influence of temperature on the dynamics of NO oxidation over the Fe- and Cu-zeolite + BaO/Al$_2$O$_3$ physical mixtures is shown in Figs. 3 and 4, respectively.

In the case of Fe-ZSM-5, Fig. 3A, a clear trend is evident: on increasing the temperature from 120 °C to 300 °C the NO concentration dip, extremely broad and almost negligible at 120 °C, becomes more and more pronounced and sharper. This can be explained considering the combination of two different effects: at higher temperatures, the NO oxidation activity is increased, as also evident from the steady state NO conversions (175 ppm at the highest temperature), while the NOx storage capacity of BaO is progressively decreased, as confirmed by integral calculations (see below), due to the greater thermal instability of the accumulated nitrites [18,20,21]. As a net result, the available
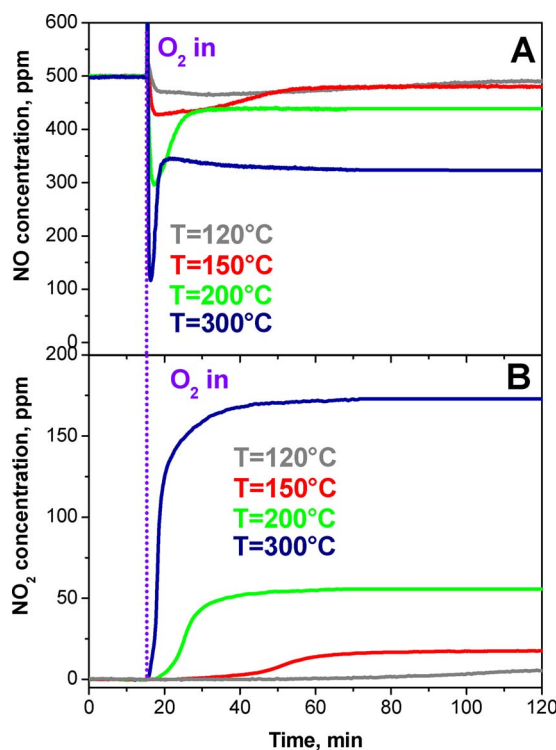

Fig. 2. O$_2$ step feed during NO isothermal adsorption (T = 150 °C; NO = 500 ppm; O$_2$ = 2%) on Cu-CHA only (dotted lines) and Cu-CHA + BaO/Al$_2$O$_3$ mechanical mixture (solid lines).

Fig. 3. O$_2$ step feed during NO isothermal adsorption (NO = 500 ppm; O$_2$ = 2%) on Fe-ZSM–5 + BaO/Al$_2$O$_3$ mechanical mixture at different temperatures: A) NO; B) NO$_2$.

Table 1
Fe-ZSM-5 containing systems: summary of integral calculations of stored (Fe-ZSM–5 + BaO/Al$_2$O$_3$ physical mixture)/reacted (Fe-ZSM-5 with preadsorbed NH$_3$) quantities at different temperatures.

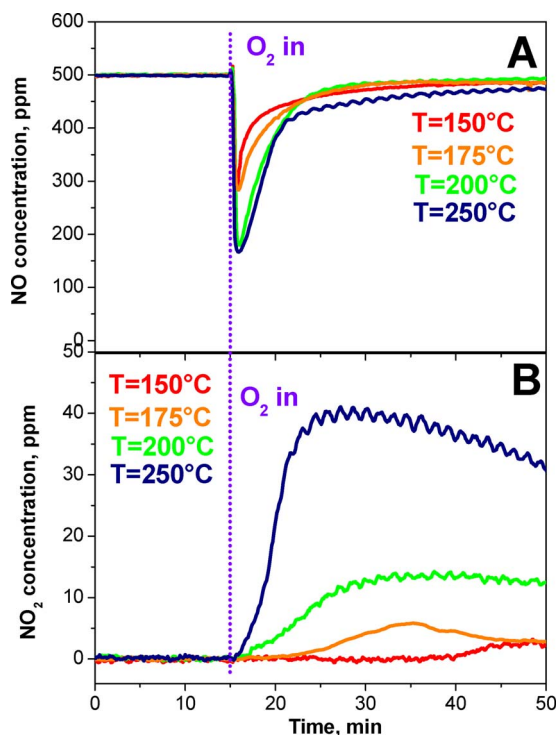|	T = 120 °C	T = 150 °C	T = 200 °C	T = 250 °C	T = 300 °C
Experiments on Fe-ZSM-5 + BaO/Al$_2$O$_3$					
NOx stored (μmol)	10.1	9.4	8.1	7.5	5.5
Experiments on Fe-ZSM-5 with preadsorbed NH$_3$					
NOx consumed (μmol)	n/a	13.5	10.6	7.4	n/a
N$_2$ produced (μmol)	n/a	16.6	10.5	6.7	n/a
NH$_3$ stored (μmol)	n/a	n/a	11.0	n/a	n/a

Fig. 4. O$_2$ step feed during NO isothermal adsorption (NO = 500 ppm; O$_2$ = 2%) on Cu-CHA + BaO/Al$_2$O$_3$ mechanical mixture at different temperatures: A) NO; B) NO$_2$.
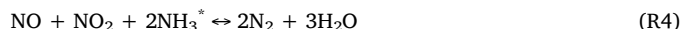
storage sites are saturated at a faster rate, resulting in progressively sharper NO dip dynamics. The overall storage of nitrites, as obtained from integral calculations according to the already described protocol, was: 10.1 μmol, 9.4 μmol, 8.1 μmol and 5.5 μmol from the lowest to the highest temperature. An overall summary of the stored/reacted quantities is reported in Table 1 below. NO$_2$ evolution (Fig. 3B) grows with increasing temperature, as expected.

Fig. 4 shows a similar set of experiments performed on the Cu-CHA sample mixed with BaO/Al$_2$O$_3$. At 150 °C and 175 °C the same extremely fast and sharp dynamics already discussed for Fig. 2 is noticed. Comparing the NO profiles at 150 °C in Figs. 3 and 4A, it is evident that NO oxidation on Cu-CHA is much faster than on Fe-ZSM-5, thus pointing out a clear role of the redox component. However, on increasing the temperature, the dip becomes deeper but also broader and with overall slower dynamics, with no significant further changes when moving from 200 °C to 250 °C. Interestingly, the transition from 150/175 °C to 200/250 °C behavior is steep and very fast, as also discussed in the last section. Fig. 4B shows on one side that the steady state NO oxidation activity increases with increasing temperature, as expected, but also evidences peculiar NO$_2$ concentration profiles, typical of the Cu-CHA containing systems. While these data and the associated dynamics are not easy to explain, if compared to those of Fe-ZSM-5 based samples, several aspects might be considered: i) the initial unconstrained NO oxidation on Cu-CHA is significantly faster than on Fe-

ZSM-5; ii) the initial oxidation rate increases with temperature, as expected; iii) the NO$_2$ inhibition is much more pronounced on Cu-CHA, as discussed in the previous section, leading to similar steady state oxidation activities, as evident in Fig. 4; iv) the nitrites stability might be different and their conversion into nitrates might proceed with different rates with respect to Fe-ZSM-5; v) at the higher temperatures (200/250 °C) the unconstrained NO oxidation is very fast on Cu-CHA: the NO dip might be so rapid and deep that its dynamics cannot be fully captured by the UV analyzer, whose temporal resolution is about 5 s. The overall storage of nitrites, as obtained from integral calculations, is: 6.1 μmol, 6.5 μmol, 8.0 μmol, 7.7 μmol from the lowest to the highest temperature. Interestingly, the amount of NOx stored at both 200 °C and 250 °C (additional test not reported for brevity) are similar to those obtained for the Fe-ZSM–5 + BaO/Al$_2$O$_3$ mechanical mixture at the same temperature (8.1 μmol and 7.5 μmol, respectively). This is a clear indication that the overall NOx storage capacity is just a function of temperature, once the load of BaO/Al$_2$O$_3$ is fixed, being essentially independent of the catalyst used. This correlation is apparently lost at lower temperature, though: e.g. 6.1 μmol on Cu-CHA vs 9.4 μmol on Fe-ZSM-5 at 150 °C. The reason is probably related to the difficulty in reaching a steady state in Cu-CHA experiments, where BaO/Al$_2$O$_3$ saturation at this temperature occurs with extremely slow dynamics, in the order of several hours. Summarizing, at low temperature, saturation of the BaO/Al$_2$O$_3$ storage capacity might not be complete on Cu-CHA, which also explains why we observe an increase in the storage with temperature. An overall summary of stored/reacted quantities is reported in Table 2 below.

3.3. Influence of preadsorbed ammonia on the NO oxidation dynamics

Fig. 5 shows the same O$_2$ step-feed experiment previously discussed, replicated at 200 °C on the Fe-ZSM-5 catalyst pre-saturated with NH$_3$. The results are surprisingly in line with those recorded on the Fe-ZSM–5 + BaO/Al$_2$O$_3$ MM mixture configuration (Fig. 1, also shown with dotted lines for comparison): the NO outlet concentration profile shows a significant dip, with a mirror evolution of N$_2$, in line with the occurrence of reactions (R2) and (R4) below:

$$NO + NO_2 + 2NH_3^* \leftrightarrow 2N_2 + 3H_2O \qquad (R4)$$

Small deviations between the two profiles can be ascribed to minor

Table 2
Cu-CHA containing systems: summary of integral calculations of stored (Cu-CHA + BaO/Al$_2$O$_3$ physical mixture)/reacted (Cu-CHA with preadsorbed NH$_3$) quantities at different temperatures.

	T = 150 °C	T = 175 °C	T = 200 °C	T = 250 °C
Experiments on Cu-CHA + BaO/Al$_2$O$_3$				
NOx stored (μmol)	6.1	6.5	8.0	7.7
Experiments on Cu-CHA with preadsorbed NH$_3$				
NOx consumed (μmol)	14.4	12.6	12.0	n/a
N$_2$ produced (μmol)	14.0	13.6	12.8	n/a
NH$_3$ stored (μmol)	15.9	n/a	n/a	n/a

Fig. 5. O$_2$ step feed during NO isothermal adsorption (T = 200 °C; NO = 500 ppm; O$_2$ = 2%) on Fe-ZSM-5 with preloaded NH$_3$ (solid lines). Fe-ZSM–5 + BaO/Al$_2$O$_3$ mechanical mixture (dotted lines) from Fig. 1 added for comparison.

differences between BaO storage sites and available adsorbed NH$_3$. Integral calculations show that the overall amount of NO converted on the system is 10.6 μmol, with 10.5 μmol of N$_2$ produced and 11 μmol of available prestored NH$_3$, estimated from a TPD experiment (not shown for brevity). Thus, adsorbed NH$_3$ apparently plays exactly the same role of the BaO-based NOx trap material in the physical mixture. Under SCR reaction conditions the products of the NO oxidative activation readily react with the adsorbed NH$_3$ to give N$_2$ and H$_2$O via ammonium nitrite decomposition: like in the chemical trapping runs, this prevents buildup of NO$_2$ in the gas phase and thus promotes an initial enhanced rate of NO oxidative activation. In principle, this indicates that, in the presence of NH$_3$, NO oxidation is significantly faster than normally measured in steady-state NO oxidation experiments, thus being potentially able to sustain the observed Standard SCR reaction rates [8].

Fig. 6 shows a similar experiment over a Cu-CHA sample pre-saturated with NH$_3$. Again, we obtain a behavior in line with the corresponding mechanical mixture configuration, with a pronounced dip in the NO outlet concentration profile, accompanied by mirror-like N$_2$ release. Notice that, differently from the Fe-ZSM-5 case, the amount of consumed NO (14.4 μmol) and thus of N$_2$ produced (14.0 μmol) is greater with respect to the NOx trapped in the MM experiment at the same temperature (6.1 μmol), in line with a higher amount of adsorbed NH$_3$ (15.9 μmol on the Cu-zeolite) if compared to the BaO/Al$_2$O$_3$ storage capacity. This might also explain the less sharp and generally slower dynamics registered in the experiment with preadsorbed NH$_3$. Interestingly, the dip is also less deep with respect to the MM case. This might indicate that preadsorbed NH$_3$, at this low temperature, could partially inhibit NO activation, slightly reducing the initial NO oxidation rate.
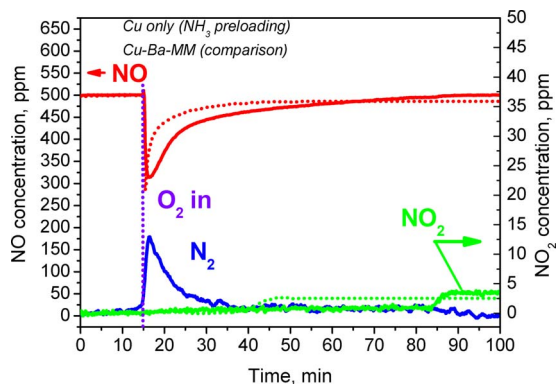

Fig. 6. O$_2$ step feed during NO isothermal adsorption (T = 150 °C; NO = 500 ppm; O$_2$ = 2%) on Cu-CHA with preloaded NH$_3$ (solid lines). Cu-CHA + BaO/Al$_2$O$_3$ mechanical mixture (dotted lines) from Fig. 2 added for comparison.

Summarizing, the present results suggest that also in Standard SCR conditions the NO oxidation may proceed with significantly faster rates than in steady-state NO oxidation runs due to self-inhibition being removed in this case by the reactivity of the generated intermediates with ammonia.

3.4. Influence of temperature on the NO oxidation dynamics in the presence of preadsorbed ammonia

Figs. 7 and 8 illustrate the influence of temperature on the NO oxidation dynamics over the two metal-promoted zeolite catalysts preloaded with NH$_3$.

On Fe-ZSM-5 (Fig. 7) a clear trend is again visible: on increasing the temperature the NO concentration dip becomes progressively more pronounced and sharp, in line with the temperature effect already discussed for the runs over the physical mixtures, see Fig. 3. In this case, being ammonia adsorbed at the temperature of the test, beside the increase in NO oxidation rate, a significant decrease in the stored ammonia can be expected with increasing temperature. The resulting combined effect is similar to what already discussed for the Fe-ZSM–5 + BaO/Al$_2$O$_3$ mechanical mixture. From integral calculations, the amount of converted NO at the different temperatures is 13.5 μmol, 10.6 μmol and 7.4 μmol while, the corresponding amount of produced N$_2$ is 16.6 μmol, 10.5 μmol and 6.7 μmol respectively. Within experimental error, these results are therefore in agreement with the stoichiometry of reactions (R2) and (R4). A summary of the overall stored/reacted quantities is reported in Table 1 above.

Fig. 8 shows the same O$_2$-step feed experiments performed at 150, 175 and 200 °C on the Cu-CHA sample preloaded with ammonia. In this case, a peculiar dynamic behavior is evident starting from 175 °C: the NO concentration trace shows a first very sharp and marked dip, which is already quite fast, followed by a second plateau, less pronounced but still distinct from the steady state conversion level. At 200 °C the situation is essentially similar with an even more evident distinction between the different dynamics. The existence of this peculiar profile with two different regions, typical of the Cu-CHA catalysts, might be related to the presence of different adsorbed NH$_3$ species with different stability, as discussed in the literature [25,26]. First, the more reactive ammonia reacts immediately with NO and NO$_2$ produced by the very rapid and uninhibited initial NO oxidation. Afterwards, and only if the temperature is sufficiently high, the more strongly adsorbed NH$_3$ can also react, originating the second plateau. The significant change in the overall NO dip dynamics when increasing the temperature from 150 °C to 200 °C could also be consistent with a reduction in the NH$_3$ inhibition of the low-temperature NO activation, as discussed previously. From integral calculations, the amount of converted NOx at the different temperatures is 14.4 μmol, 12.6 μmol and 12.0 μmol while, the amount of produced N$_2$ is 14.0 μmol, 13.6 μmol and 12.8 μmol respectively. Within experimental error, these results are in line with the stoichiometry of reactions (R2) and (R4). A summary of the overall stored/reacted quantities is reported in Table 2 above.

3.5. Relevance for the standard SCR activity

At this point, we proceed to discuss the relevance of our findings for the catalytic mechanism of the Standard SCR reaction. To this purpose, Figs. 9 and 10A compare NO conversions measured at the lowest point of the NO concentration dip (both in the presence of BaO and of preadsorbed ammonia) with steady-state NO conversions from Standard SCR and NO oxidation tests on the metal promoted-zeolite (Cu-CHA and Fe-ZSM-5) catalysts in similar conditions. In these plots, the conversion profiles of the NO to NO$_2$ oxidation runs have been multiplied by two to challenge the hypothesis that both Standard SCR and NOx trapping by BaO or by adsorbed NH$_3$ may be explained by the two-step sequential scheme obtained by considering reactions (R2) + (R3) or (R2) + (R4), respectively, occurring in series. In fact, according to this simplified
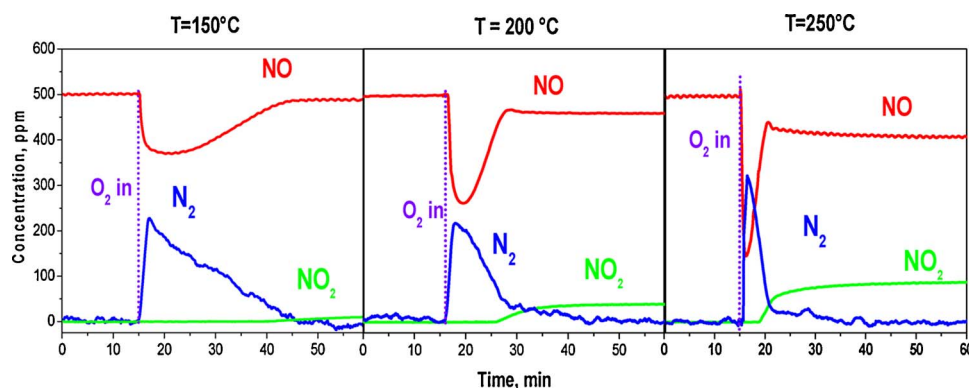
Fig. 7. O_2 step feed during NO isothermal adsorption (NO = 500 ppm; O_2 = 2%) on Fe-ZSM-5 with pre-loaded NH_3 at different temperatures. T = 200 °C added for comparison (Fig. 5).

Standard SCR mechanism, NO is firstly oxidized to NO_2 and then one additional NO molecule reacts with NO_2 and NH_3 in a fast step: in this respect, it is relevant to compare the NO conversion in Standard SCR conditions with the NO conversion in steady state NO oxidation multiplied by two. Figs. 9 and 10A provide, thus, a fair comparison of the rates of NO conversion to NO_2 in the different tested conditions, under the assumption that neither the storage of NO + NO_2 on BaO/Al_2O_3 nor their reaction with NH_3 is rate limiting.

In addition, Figs. 9B and 10B show the transient Standard SCR activities for different concentration levels of gas-phase NH_3. All the experiments were carried out feeding a volumetric flow rate of 120 cm^3/min (STP), 2% O_2, 500 ppm of NO and 500/250 or 100 ppm of NH_3 (when present) under dry conditions. In fact, as already discussed in the experimental section, previous works pointed out a strong negative impact of H_2O on the amount of NOx trapped on BaO, due to its inhibitory action both on the NO oxidation activity of metal promoted zeolites [23], and on the nitrites storage on BaO [21].

Fig. 9A shows the results for the Cu-CHA based systems. In this case, the steady-state NO oxidation activity to NO_2 (orange line) is extremely limited and clearly unable to sustain the Standard SCR activity (blue line), as expected [8]. Interestingly, once BaO/Al_2O_3 is added to Cu-CHA, the initial NO oxidation activity is strongly improved (green line), as already discussed, overcoming significantly the Standard SCR activity at all the tested temperatures: this is consistent with the existence of a strong NO_2 inhibition on the NO oxidation reaction. Similar results are obtained with preadsorbed NH_3 (red line): the initial NO conversion (oxidation) is improved and, if we consider the not perfect equivalence between BaO storage sites and adsorbed ammonia, the situation is well comparable to the case of the mechanical mixture. It is interesting to notice the different trends as a function of T in the dip dynamics of the two systems. Apparently, NOx removal by BaO is enhanced once a critical temperature that lies between 175 °C and 200 °C is reached, while the NH_3 trapping has a maximum at 175 °C and then decreases, probably due to the reduced ammonia storage with rising temperature. The NH_3 related result may be somehow surprising if compared to the steady-state Standard SCR activity. In principle, one can expect that

there should be no difference between the maximum NO conversion over the Cu-CHA sample with preloaded ammonia and in steady-state Standard SCR runs, since the NO_2 inhibition on the NO oxidative activation would be equally absent. This however is not exactly true, as evident from the experimental results, and might be due to additional NH_3 inhibition effect in Standard SCR. Indeed, on inspecting Fig. 9B it is clear that by progressively reducing the NH_3 present in the gas phase (at a given temperature, in this case 150 °C) we are incrementing the NO conversion in the steady-state Standard SCR test, closer to the ones measured in transient tests with preadsorbed NH_3. It can be argued that even at low NH_3 concentrations (125 ppm) we are significantly far from the NO conversions obtained in the dip experiments with preloaded NH_3. However, it is evident how, in transient conditions, NO conversion can reach higher values with respect to what happens at steady-state (up to 22% approximately); getting closer to the NO dip situation. This suggests that the best Standard SCR performances are achieved when a high amount of adsorbed ammonia is available and, at the same time, the gas phase NH_3 concentration is minimal.

Summarizing, in this case, two clear inhibiting effects can be noticed, at least at low temperature: i) NO_2 presence in the gas phase strongly reduces the NO oxidative activation rate; ii) NH_3 presence in the gas phase can reduce the maximum achievable NO conversions in Standard SCR, especially when compared to the ammonia preloaded case. On Cu-CHA however, the NH_3 inhibition effect is significantly reduced as soon as the temperature is increased above 200 °C (blue and red lines converging in Fig. 9A) and is generally less pronounced than over Fe-ZSM-5 (see below). This is in line with many studies in the literature [27,28] claiming that the NH_3 inhibition of Standard SCR is less significant on Cu-zeolite catalysts. Nevertheless, the observation of a limited inhibition of Standard SCR by gas phase NH_3 may be relevant to the ongoing discussion on the formation of transient Cu dimers in presence of NH_3 in Cu-CHA catalysts, as reported, for example in [15,29].

Fig. 10A–B shows the same experiments of Fig. 9 for the Fe-ZSM-5 based systems. Here, at the same experimental conditions and in the absence of H_2O, NO conversions in steady-state oxidation tests
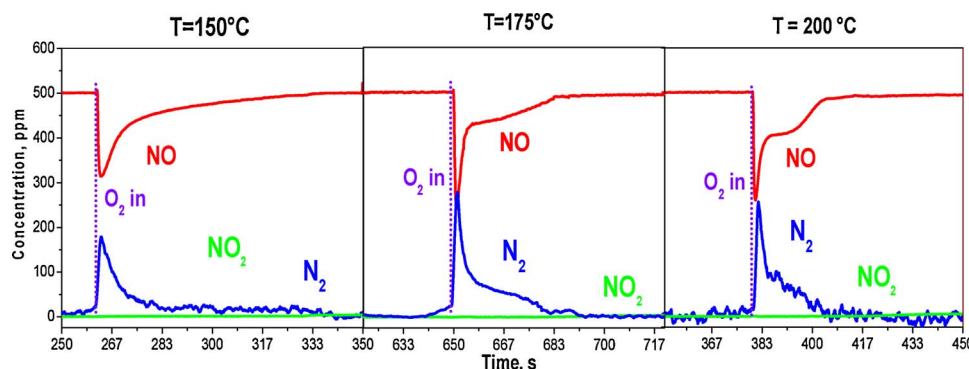

Fig. 8. O_2 step feed during NO isothermal adsorption (NO = 500 ppm; O_2 = 2%) on Cu-CHA with pre-loaded NH_3 at different temperatures. T = 150 °C added from comparison (Fig. 6).
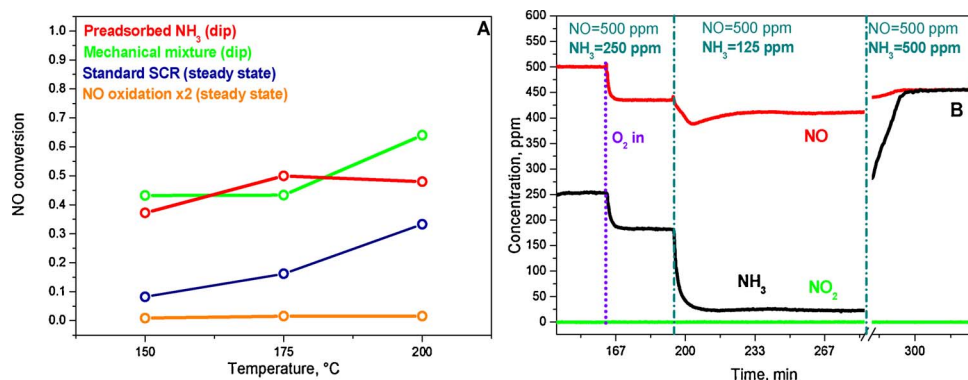
Fig. 9. Cu-CHA containing systems. A) NO conversion in different experiments as a function of feed temperature; B) transient NO conversion in reference Standard SCR experiment (Q = 120 Ncc/min, O_2 = 2%, T = 150 °C. NO = 500 ppm) as a function of NH_3 concentration in the gas phase (NH_3 = 500/250/125 ppm).

multiplied by 2 (orange line) essentially match the NO conversions in Standard SCR (blue line), at least at the lower temperatures. Apparently, this suggests that, in absence of H_2O, the NO oxidation activity of this Fe-ZSM-5 catalyst is sufficient to sustain the Standard SCR activity. This result is somehow in line with our previous findings [8] and with what reported in the literature and already discussed in the Introduction: at the same (dry) conditions, the rate of NO oxidation to NO_2 on Fe zeolites may be similar or even overcome the rate of Standard SCR [8,17]. At this point, however, different aspects must be considered: (i) the effect of H_2O is in general significantly different in the two cases, with a strong inhibition of the NO oxidation and a more limited effect on the Standard SCR activity, as also reported in [8]; (ii) the NO oxidation and Standard SCR activities, and their relative ratios, can be different depending on the type of Fe-zeolite catalyst and on the adopted preparation method, as discussed in [30,31]; (iii) NH_3 inhibition, more significant in the case of Fe-catalysts as highlighted in Fig. 10B, can play an important role in determining the actual NO oxidation rate under reaction conditions. Indeed, Fig. 10B points out that, on progressively reducing the gas phase NH_3 concentration, the NO conversion can reach higher values with respect to steady-state (up to 30% approximately), thus approaching the NO dip level. It is important to notice that, like in the case of Cu-CHA, as soon as NO_2 is effectively removed from the gas phase (by either BaO or preadsorbed NH_3), the NO oxidative activation is greatly boosted, largely overcoming the Standard SCR activity at the lower temperatures.

Comparing Figs. 9A and 10A, it can be noticed that, despite Cu-CHA is significantly more active than Fe-ZSM-5 in the unconstrained NO oxidation, it is also much more inhibited by NO_2 at steady state, as already pointed out. If the NO_2 inhibition is due to formation of nitrates blocking the Cu sites, as proposed in the literature [4,32], this observation might be in line with the different stability of nitrates on the two catalysts, as shown by dedicated Temperature Programmed Desorption and Temperature Programmed Surface Reaction tests in Fig. 11A–B below. Prior to these experiments, the two catalysts were saturated with nitrates (not shown) by feeding 500 ppm of NO_2 and 8%

O_2 at 120 °C. Then, in Fig. 11A, the temperature was progressively increased at 15 °C/min in an inert flow of He to assess thermal stability of the stored NOx species, while in Fig. 11B, the NOx adspecies were exposed to 500 ppm of NO in He during an initial isothermal stage (at 120 °C), followed by a temperature ramp with the same heating rate. It is evident that, on Cu-CHA, nitrates are more thermally stable as well as more difficult to reduce than on Fe-ZSM-5: in particular, NO reduced all the stored nitrates already at 120 °C on the Fe-zeolite, whereas nitrates were still present on the Cu-zeolite catalyst after exposure to NO at the same temperature, and their reduction was completed only at 400 °C. The greater stability and lower reactivity of nitrates on Cu-CHA could possibly result in a stronger inhibitory effect of NO_2 with respect to Fe-ZSM-5. It should be mentioned however that these results and the related interpretation are at variance with [33], where no residual presence of stable adsorbed nitrates was detected on Cu-CHA catalysts in the presence of gas phase NO. As a matter of fact, NO oxidation might also be kinetically hindered directly by its gas phase products (NO_2), as also discussed in literature [2,24].

4. Conclusions

We have shown that in physical mixtures comprising a metal-promoted zeolite catalyst (Fe-ZSM-5, Cu-CHA) and a NOx storage material (BaO/Al_2O_3), the low-temperature oxidative activation of NO is greatly enhanced as long as BaO can efficiently remove the inhibiting NO oxidation products (such as NO_2 or HONO/N_2O_3) from the gas phase, storing them in the form of Ba nitrites. The very same behavior is observed when the NOx storage phase, BaO/Al_2O_3, is replaced by ammonia preadsorbed on the metal zeolite: in this case the gaseous NO oxidation products are likewise effectively removed from the gas phase, being rapidly converted to dinitrogen. This suggests that in Standard SCR conditions the real NO oxidation activity of metal promoted zeolite catalysts can be much higher than expected from steady-state NO oxidation tests. This is particularly significant for Cu-CHA, which shows an initial 40–fold activity improvement over steady-state NO to NO_2
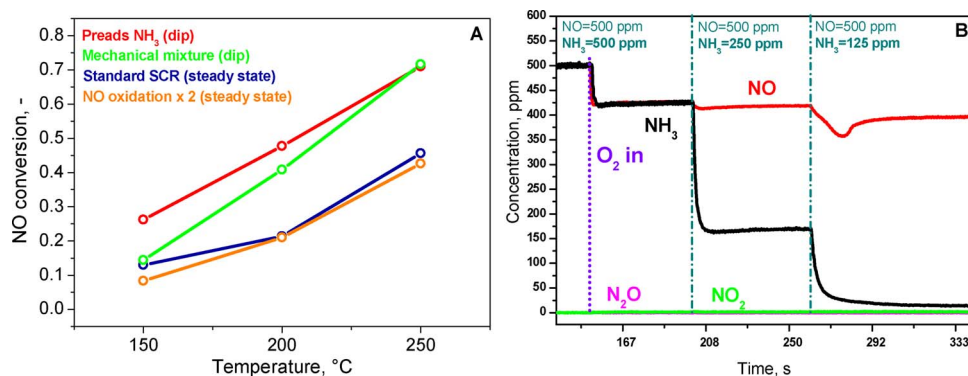

Fig. 10. Fe-ZSM-5 containing samples. A) NO conversion in different experiments as a function of feed temperature; B) transient NO conversion in reference Standard SCR experiment (Q = 120 Ncc/min, O_2 = 2%, T = 200 °C. NO = 500 ppm) as a function of NH_3 content in the gas phase (NH_3 = 500/250/125 ppm).
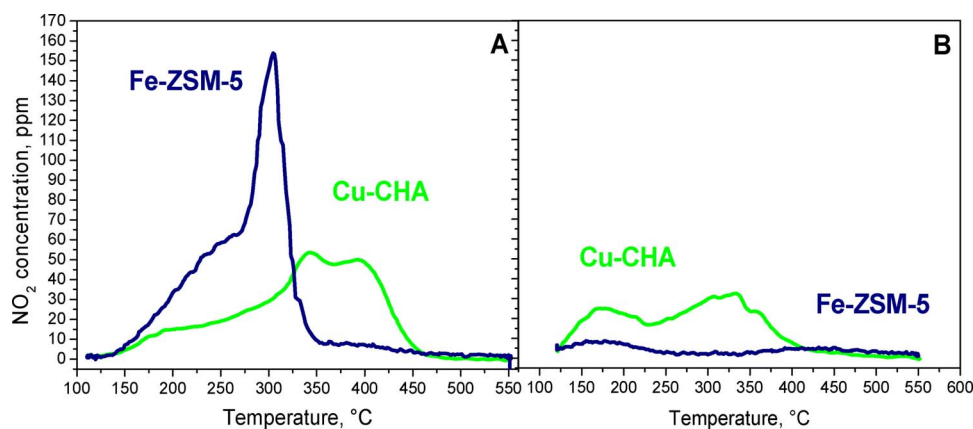
Fig. 11. (A) TPD runs in He (T = 120–550 °C; heating rate = 15 °C/min); B) TPSR run in NO (NO = 500 ppm, T = 120–550 °C; heating rate = 15 °C/min) following $NO_2 + O_2$ adsorption at 120 °C (NO_2 = 500 ppm; O_2 = 8%) on: Fe-ZSM-5 and Cu-CHA.

oxidation conditions at 150 °C. The direct comparison with the Standard SCR activity at low temperature, however, is complicated by the NH_3 inhibition observed both over Cu-CHA and particularly over Fe-ZSM-5.

References

[1] M. Devadas, O. Kröcher, M. Elsener, A. Wokaun, N. Söger, M. Pfeifer, Y. Demel, L. Mussmann, Appl. Catal. B: Environ. 67 (2006) 187–196.

[2] P.S. Metkar, N. Salazar, R. Muncrief, V. Balakotaiah, M.P. Harold, Appl. Catal. B: Environ. 104 (2011) 110–126.

[3] M. Iwasaki, K. Yamazaki, H. Shinjoh, Appl. Catal. A: Gen. 366 (2009) 84–92.

[4] H. Sjövall, R.J. Blint, L. Olsson, Appl. Catal. B: Environ. 92 (2009) 138–153.

[5] A.Y. Stakheev, A.I. Mytareva, D.A. Bokarev, G.N. Baeva, D.S. Krivoruchenko, A.L. Kustov, M. Grill, J.R. Thøgersen, Catal. Today 258 (Part 1) (2015) 183–189.

[6] Q. Sun, Z.-X. Gao, H.-Y. Chen, W.M.H. Sachtler, J. Catal. 201 (2001) 89–99.

[7] M. Richter, R. Eckelt, B. Parlitz, R. Fricke, Appl. Catal. B: Environ. 15 (1998) 129–146.

[8] M.P. Ruggeri, I. Nova, E. Tronconi, Top. Catal. 56 (2013) 109–113.

[9] J.H. Kwak, J.H. Lee, S.D. Burton, A.S. Lipton, C.H.F. Peden, J. Szanyi, Angew. Chem. – Int. Ed. 52 (2013) 9985–9989.

[10] F. Gao, J.H. Kwak, J. Szanyi, C.H.F. Peden, Top. Catal. 56 (2013) 1441–1459.

[11] C. Paolucci, A.A. Verma, S.A. Bates, V.F. Kispersky, J.T. Miller, R. Gounder, W.N. Delgass, F.H. Ribeiro, W.F. Schneider, Angew. Chem. (2014) 11828–11833.

[12] T.V.W. Janssens, H. Falsig, L.F. Lundegaard, P.N.R. Vennestrøm, S.B. Rasmussen, P.G. Moses, F. Giordanino, E. Borfecchia, K.A. Lomachenko, C. Lamberti, S. Bordiga, A. Godiksen, S. Mossin, P. Beato, ACS Catal. 5 (2015) 2832–2845.

[13] C. Paolucci, A.A. Parekh, I. Khurana, J.R. Di Iorio, H. Li, J.D. Albarracin Caballero, A.J. Shih, T. Anggara, W.N. Delgass, J.T. Miller, F.H. Ribeiro, R. Gounder, W.F. Schneider, J. Am. Chem. Soc. 138 (2016) 6028–6048.

[14] D.E. Doronkin, M. Casapu, T. Günter, O. Müller, R. Frahm, J.-D. Grunwaldt, J. Phys. Chem. C 118 (2014) 10204–10212.

[15] F. Gao, D. Mei, Y. Wang, J. Szanyi, C.H.F. Peden, J. Am. Chem. Soc. 139 (2017) 4935–4942.

[16] R.Q. Long, R.T. Yang, J. Catal. 207 (2002) 224–231.

[17] J.H. Kwak, D. Tran, J. Szanyi, C.H.F. Peden, J.H. Lee, Catal. Lett. 142 (2012) 295–301.

[18] T. Selleri, I. Nova, E. Tronconi, Appl. Catal. B: Environ. 206 (2017) 471–478.

[19] B.M. Weiss, K.B. Caldwell, E. Iglesia, J. Phys. Chem. C 115 (2011) 6561–6570.

[20] M.P. Ruggeri, T. Selleri, M. Colombo, I. Nova, E. Tronconi, J. Catal. 311 (2014) 266–270.

[21] M.P. Ruggeri, T. Selleri, M. Colombo, I. Nova, E. Tronconi, J. Catal. 328 (2015) 258–269.

[22] T. Selleri, M.P. Ruggeri, I. Nova, E. Tronconi, Top. Catal. 59 (2016) 678–685.

[23] A. Grossale, I. Nova, E. Tronconi, Catal. Today 136 (2008) 18–27.

[24] B.M. Weiss, E. Iglesia, J. Phys. Chem. C 113 (2009) 13331–13340.

[25] I. Lezcano-Gonzalez, U. Deka, B. Arstad, A. Van Yperen-De Deyne, K. Hemelsoet, M. Waroquier, V. Van Speybroeck, B.M. Weckhuysen, A.M. Beale, Phys. Chem. Chem. Phys. 16 (2014) 1639–1650.

[26] D. Wang, L. Zhang, K. Kamasamudram, W.S. Epling, ACS Catal. 3 (2013) 871–881.

[27] A. Grossale, I. Nova, E. Tronconi, D. Chatterjee, M. Weibel, Top. Catal. 52 (2009) 1837.

[28] P.S. Metkar, M.P. Harold, V. Balakotaiah, Chem. Eng. Sci. 87 (2013) 51–66.

[29] C. Paolucci, I. Khurana, A.A. Parekh, S. Li, A.J. Shih, H. Li, J.R. Di Iorio, J.D. Albarracin-Caballero, A. Yezerets, J.T. Miller, W.N. Delgass, F.H. Ribeiro, W.F. Schneider, R. Gounder, Science 357 (2017) 898–903.

[30] G. Delahay, D. Valade, A. Guzmán-Vargas, B. Coq, Appl. Catal. B: Environ. 55 (2005) 149–155.

[31] I. Ellmers, R.P. Vélez, U. Bentrup, A. Brückner, W. Grünert, J. Catal. 311 (2014) 199–211.

[32] P.S. Metkar, V. Balakotaiah, M.P. Harold, Catal. Today 184 (2012) 115–128.

[33] H.-Y. Chen, Z. Wei, M. Kollar, F. Gao, Y. Wang, J. Szanyi, C.H.F. Peden, Catal. Today 267 (2016) 17–27.